

# Orbifold Train Tracks on Simple Hyperbolic Braids

Yandi Wu

August 6, 2018

Advisors: Ian Agol, Carolyn Abbott

*Abstract.* Agol proves the eventual periodicity of a maximal splitting sequence of a train track obtained from the stable lamination of a pseudo-Anosov homeomorphism. We generalize this result to orbifolds obtained from taking quotients of  $k$ -holed spheres by isometries in  $\mathbb{R}^n$ .

## 1 Introduction

Farb, Leininger, and Margalit prove the existence of a finite collection of fibered hyperbolic 3-manifolds such that every small-dilatation pseudo-Anosov is a monodromy of a mapping torus that can be obtained by a Dehn filling on a member of the finite collection [1]. In [2], Ian Agol reproved the theorem using ideal triangulations of mapping tori of pseudo-Anosov maps and maximal splitting sequences of train tracks. The Agol maximal splitting sequence does not allow isolated monogons. As a result, train tracks described in Agol's paper are rather different from, and in fact may prove more complex than, the splitting sequences described by Kin and Hironaka [3]. By examining train tracks with isolated monogons, this expository piece is a step towards reconciling differences between Agol's splitting sequence and the Hironaka-Kin sequence. We also explore Agol's theorem with simple orbifolds.

*Acknowledgements:* I would like to thank my advisors: Ian Agol for suggesting this project, which is completely full of his ideas, and offering pragmatic but encouraging life advice along the way, and Carolyn Abbott for her guidance, which was crucial to this project, moral support, and decryptions of Professor Agol's suggestions. Additionally, I'd like to thank Nic Brody for answering my copious questions both in person and over email and editing a draft of this writeup. I would also like to thank Dan Margalit and Balázs Strenner, who introduced me to geometric group theory and continue to inspire me with their work and dedication to mentoring. Finally, I'd like to thank Alex Appleton and Joe Stahl for answering every math question I had and both encouraging and feeding into my addiction to math.

## 2 Definitions

### 2.1 Orbifolds

We define orbifolds in a way that suffices for the purposes of this discussion. Note this definition does not work for "bad" orbifolds such as the teardrop orbifold, which do not have manifold covers. Let  $\Gamma$  be a discrete isometry in  $\mathbb{R}^n$  and  $S \subseteq \mathbb{R}^n$  a submanifold invariant under  $\Gamma$ . Then  $S/\Gamma$  is an *orbifold*. If  $\Gamma$  has no fixed points, then  $S/\Gamma$  is a manifold.

We provide some simple examples. Suppose  $\Lambda = \langle (x, y) \mapsto (x + 1, y), (x, y) \mapsto (x, y + 1) \rangle \cong \mathbb{Z}^2$ , which gives a tessellation of  $\mathbb{R}^2$ , effectively tiling it. There are no fixed points as  $\Lambda$  describes translations. Note that  $\mathbb{R}^2/\Lambda \cong T^2$ , since  $\Lambda$  describes the gluing map of a torus, a manifold. Now let  $\Gamma$  describe a tessellation on  $\mathbb{R}^2$  with fixed points, for example rotations by  $\pi$ . Then  $\Gamma$  is cyclic of order 2, so  $\Gamma \cong \mathbb{Z}/2\mathbb{Z}$ . Consider  $(\mathbb{R}^2/\Lambda)/\Gamma$ , or the quotient of the torus by the hyperelliptic involution. The resulting orbifold is a pillowcase (see figure 1).

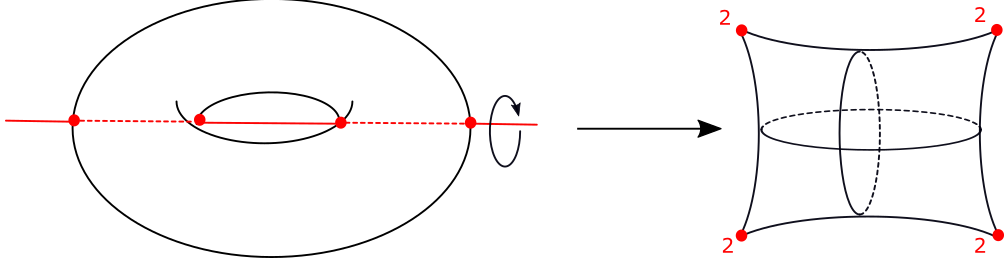


Figure 1: An example of a orbifold obtained by taking the quotient of the torus.

The orbifolds we deal with in this paper can be visualized as spheres with a finite number of cone points, each labeled with with an integer  $n$  specifying the order of  $\Gamma$ . In the aforementioned case, all four cone points are labeled with 2, specifying the group action under question is  $\mathbb{Z}/2\mathbb{Z}$ .

## 2.2 Branched Covers

Recall that a space  $\tilde{X}$ , along with a map  $p$  from  $\tilde{X}$  to the base space  $X$ , is a covering space of  $X$  if every point in  $X$  has an open neighborhood  $\mathcal{U}$  whose preimage is a disjoint union of open sets in  $\tilde{X}$ . Furthermore, each member of this disjoint union maps homeomorphically onto  $\mathcal{U}$ . If  $X$  is evenly covered, a *sheet* is one homeomorphic copy of the open sets in  $p^{-1}(\mathcal{U})$ . If there are two sheets mapping homeomorphically to  $\mathcal{U}$ , then we say  $\tilde{X}$  is a *double cover* of  $X$ . Suppose that with the exception of a finite number of *branch points* in  $\tilde{X}$  that do not map homeomorphically onto any neighborhood in  $X$ ,  $\tilde{X}$  is a cover of  $X$ . Then  $\tilde{X}$  is a *branched cover* of  $X$ .

For example, consider the wedge sum of two circles.  $S^1 \vee S^1$  is a branched double cover of  $S^1$  since no neighborhood of the intersection point  $s$  of the two circles maps homeomorphically to any open set in  $S^1$ . The branch point of the cover is  $s$ . To give another example, a torus is a doubled branched cover of  $(\mathbb{R}^2/\Lambda)/\Gamma$ . The branch points,  $P = \{p_1, p_2, p_3, p_4\}$ , are fixed under hyperelliptic involution, which is consistent with our description of  $(\mathbb{R}^2/\Lambda)/\Gamma$  as an orbifold. In particular,  $P \cup S_{0,4} = (\mathbb{R}^2/\Lambda)/\Gamma$ , so we could also say the torus is a branched double cover of  $S_{0,4}$ .

## 2.3 Train Tracks and Operations

Suppose  $\Sigma = S/\Gamma$  is a surface with no boundary equipped with a hyperbolic metric (a complete metric with constant negative curvature). A (*geodesic*) *lamination*  $\mathcal{L}$  of  $\Sigma$  is a set of disjoint, non-self-intersecting, locally length-minimizing arcs, called geodesics, whose union forms a closed subset of  $\Sigma$ . The geodesics are referred to as the *leaves* of  $\mathcal{L}$ . When lifted to the universal cover, the complementary regions of  $\mathcal{L}$  consist of ideal polygons.

Recall the Nielsen-Thurston Classification Theorem of surface homeomorphisms. Given a homeomorphism on an orientable surface  $\varphi : \Sigma \rightarrow \Sigma$ , up to homotopy,  $\varphi$  is periodic, finite-order, or pseudo-Anosov. We focus on pseudo-Anosov homeomorphisms. Informally, a pseudo-Anosov homeomorphism stretches every curve on a surface exponentially. More precisely, a map  $\varphi$  is pseudo-Anosov if there exists a transverse pair of stable and unstable laminations on  $\Sigma$ , denoted  $\mathcal{L}^s$  and  $\mathcal{L}^u$  respectively, such that  $\varphi$  scales  $\mathcal{L}^s$  by some real number  $\lambda_\varphi > 1$  and  $\mathcal{L}^u$  by  $\lambda_\varphi^{-1}$ . We call  $\lambda_\varphi$  the *stretch factor* of  $\varphi$ . Laminations are often complicated to visualize. As a result, Thurston devised a combinatorial technique, a train track, for representing a lamination.

Let  $\Sigma$  be an orientable surface. A *train track*  $\tau \subset \Sigma$  is a one-complex embedded in  $\Sigma$  satisfying some extra conditions:

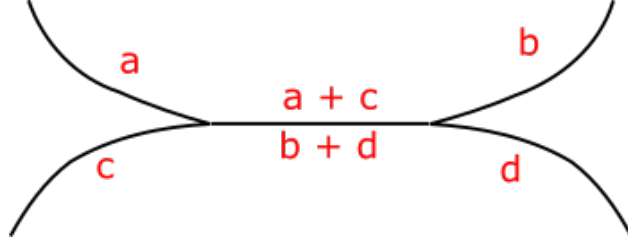


Figure 2: The switch condition requires the sum of the weights of the two sides of the switch to be equal. As a consequence, for the train track above, we have that  $a + c = b + d$ .

1. Each vertex, called a *switch*, of  $\tau$  has a well-defined tangent line.
2. Each of the edges, or *branches*, is weighted by a positive measure, and the *switch condition* (figure 2) is satisfied.

One can approximate the lamination  $\mathcal{L}$  associated with a pseudo-Anosov map  $\varphi : \Sigma \rightarrow \Sigma$  using train tracks by finding a differentiable map  $f : \Sigma \rightarrow \Sigma, \mathcal{L} \mapsto \tau$  homotopic to the identity. If  $\tau$  approximates  $\mathcal{L}$ , we say that  $\mathcal{L}$  is *suited* to  $\tau$  via the *carrying map*  $f$ .

All train tracks considered in this paper are *trivalent*, meaning each switch has three branches adjacent to it. Each branch can be divided into two half-branches, one for each end of the branch. If a half branch is on the same side of a switch as another half branch, then we call it *small*. Otherwise, a half branch is a *large half-branch*. If the two ends of a branch are large half-branches, then we call it a *large branch*. On the other hand, if the two ends of a branch are both small, we call it a *small branch*, and a *mixed branch* is comprised of one small and one large half branch.

There are three operations one can perform on train tracks: splitting, folding (see figure 3), and shifting (see figure 4). Notice that splitting only occurs on large branches, folding on small branches, and shifting on mixed branches. Recall that two embeddings connected by a continuous path of embeddings are isotopic. Since train tracks are embedded into a surface, one can talk about isotopic train tracks. We say that two train tracks are *equivalent* if, up to isotopy, they differ by a sequence of splits, folds, and shifts.

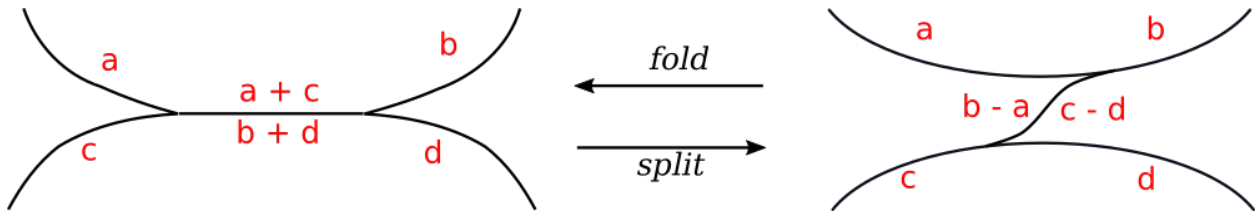


Figure 3: Splitting a large branch of a train track. Its inverse operation, a fold, occurs on a small branch.

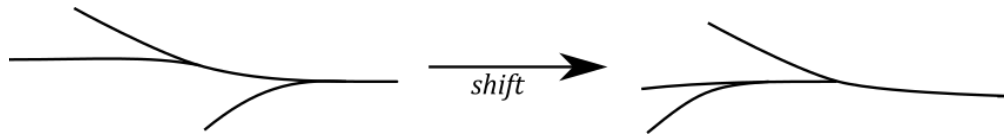


Figure 4: Shifting a mixed branch of a train track.

### 3 Orbifold Train Tracks and Operations

We can also define train tracks on orbifolds. Notice that in the branched double cover of  $(\mathbb{R}^2/\Lambda)/\Gamma$ , the torus, the singular points  $P$  lift to bigons, each with point fixed under  $\Gamma$  in the middle. In theory, we could lift  $\tau$  to the branched double cover, which is a manifold and thus has well-defined operations (ie splitting, folding, and shifting), and determine the corresponding operations on the orbifold by projecting back down (see figure 5). As illustrated in the figure, the lift of an isolated monogon is a isolated bigon. If we apply a split to the large branches adjacent to the bigon and then apply a shift by collapsing neighboring cusps, we obtain an isolated bigon sandwiched between two pairs of mixed branches. We can project this isolated bigon back downstairs to visualize the result of the action of a split-shift operation on the orbifold.

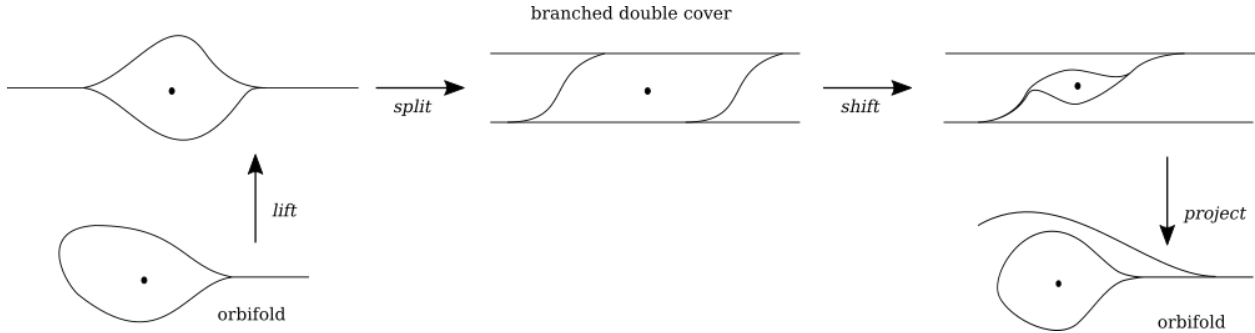


Figure 5: We can perform train track operations on the manifold double cover of an orbifold to determine operations downstairs on the orbifold itself.

However, in practice, this is complicated by the fact that although  $S_{0,4}$  has a canonical branched double cover, the torus, if we increase the number of holes, there is no such canonical cover. We work with  $S_{0,5}$  to address this issue. If we consider a train track on  $\tau \subset S_{0,5}$  where  $\tau$  has an isolated monogon around each of the punctures,  $\tau \subset (\mathbb{R}^2/\Lambda)/\Gamma$  has no monogons since  $(\mathbb{R}^2/\Lambda)/\Gamma$  has no punctures. Instead, the monogons become the branch points (see figure 6).

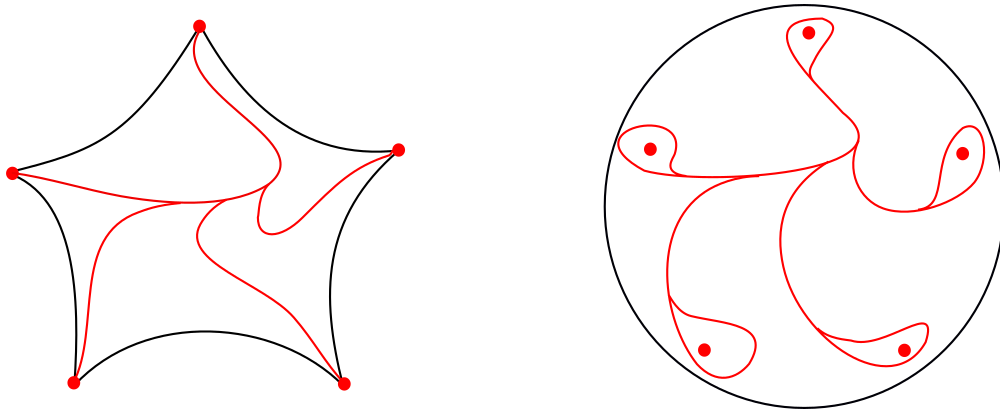


Figure 6: A monogon tree train track on an orbifold with 5 cone points can be compared to one on  $S_{0,5}$ .

Evidently, operations of train tracks with monogons are easier to visualize than ones on train tracks with orbifold points. One could easily take a train track on an orbifold, omit its  $n$  orbifold points to obtain the  $n$ -holed sphere, and visualize the same train track on  $S_{0,n}$ . In this way, we can determine the split and fold operations of orbifold train tracks (ie, see 7). This process can be further simplified by defining orbifold

train tracks in a way that allows for monogons around orbifold points. This definition could, in a way, be justified by how the fundamental group of an orbifold is defined.

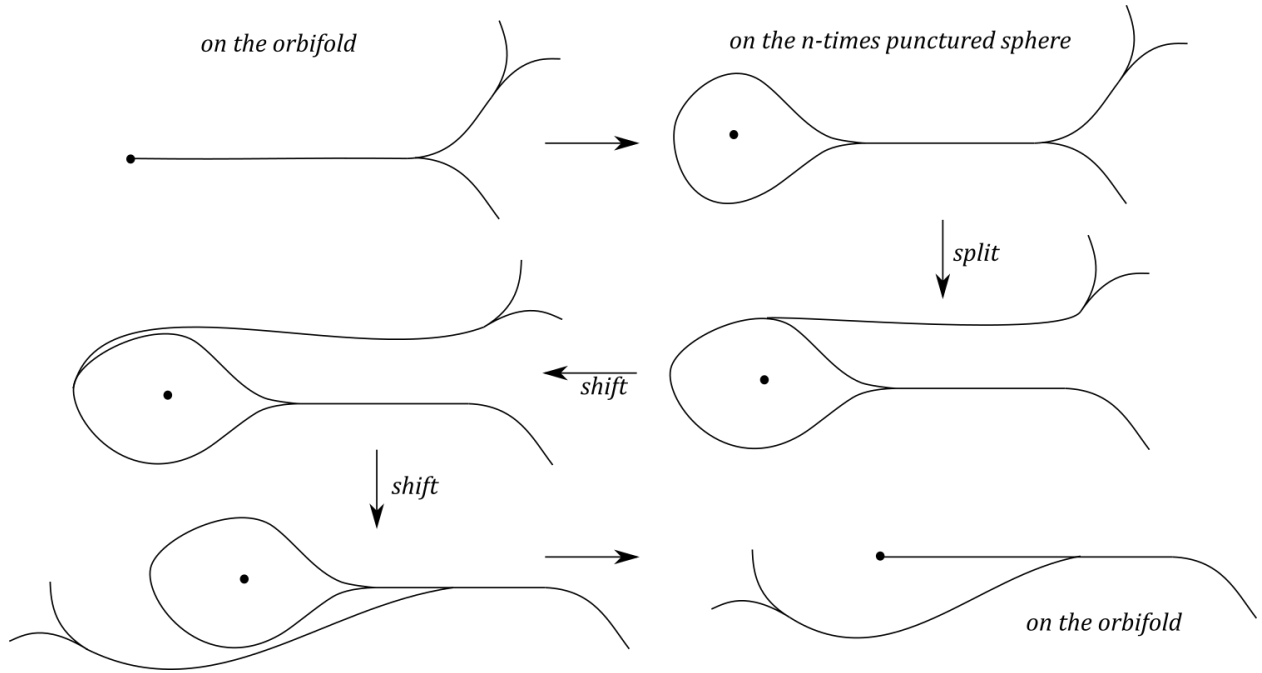


Figure 7: In order to define a split-shift sequence, one can visualize the orbifold train track by replacing the cone points with monogons and performing the desired operations on  $S_{0,n}$ .

We provide an intuitive sketch behind the definition of the fundamental group of orbifolds, based on Dan Peterson's view from [4]. Take a cone point  $p$  of order  $n$ . The point is that  $p$  is an intermediate between a point and a puncture. It is not exactly a point since the union of  $p$  with  $n$  copies of itself constitutes a point. At the same time, one cannot call  $p$  a puncture, obtained by omitting a point from a surface; however, the higher the order of  $p$ , the more analogous it is to a puncture. As a result, if one draws a loop  $\gamma$  around  $p$ , one cannot collapse  $\gamma$  down to  $p$  since  $p$  is not a proper point. However, consider the loop  $\gamma^n$ , obtained by traveling  $n$  times around  $\gamma$ , and thus  $n$  times around  $p$ . Then  $\gamma^n$  is contractible and homotopy equivalent to the trivial loop. From this perspective, one can consider  $\gamma$  to be a nontrivial element of  $\pi_1(S/\Gamma)$ , where  $S/\Gamma$  is an orbifold. As a result, a train track on  $S/\Gamma$  will contain monogons, at least in the case we are considering, around each cone point.

## 4 Periodic maximal splitting sequences of orbifold train tracks

### 4.1 Notation

The notation of this paper is, for the most part, consistent with Agol's. We denote a split of a measured train track by  $(\tau, \mu) \prec (\tau', \mu')$ . If a split occurs along a specified large branch  $e \subset \tau$ , we write  $(\tau, \mu) \overset{e}{\prec} (\tau', \mu')$ . We define a *maximal splitting* as a split along the branch of maximal weight. If there are multiple branches of maximal weight, all of them are split simultaneously.  $(\tau, \mu) \overset{n}{\prec} (\tau', \mu')$  denotes a sequence of  $n$  maximal splits. If the number of maximal splits is unspecified, then I write  $(\tau, \mu) \overset{max}{\prec} (\tau', \mu')$ .

## 4.2 Penner-Harer's Theorems

We provide two fundamental statements that are crucial to our final results, taken from Theorem 2.8.5 of [5]. The following facts are true in the manifold case; we want to show the results carry over to the case of well-behaved orbifolds.

**Theorem 4.1.** *If a lamination  $\mathcal{L}$  is suited to two measured train tracks  $(\tau, \mu)$  and  $(\tau', \mu')$ , then  $(\tau, \mu) \sim (\tau', \mu')$ .*

**Theorem 4.2.** *If  $\mathcal{L}$  is suited to  $(\tau, \mu)$  and  $(\tau, \mu) \sim (\tau', \mu')$ , then  $\mathcal{L}$  is suited to  $(\tau', \mu')$  as well.*

Although a rigorous proof of these two theorems is beyond the scope of this paper, we provide a sketch of one proof, which utilizes Fenchel-Nielsen coordinates. Other potential directions in proving the theorem involve standard train tracks on surfaces (see [5]) and the more combinatorial approach of ideal triangulations introduced by Marc Lackenby [6].

### 4.2.1 Fenchel-Nielsen Coordinates

We now define Fenchel-Nielsen coordinates, sweeping a few details under the rug and taking many facts for granted. Most of this information is based on Feng Zhu's notes on hyperbolic geometry [7].

The *Teichmüller space* of a hyperbolic surface  $\Sigma = \Sigma_{g,0}$ , denoted  $\mathcal{T}(\Sigma)$ , is a collection of equivalence classes of marked hyperbolic metrics. By the Uniformization Theorem, there is a bijection between hyperbolic metrics and Riemann surface structures, so  $\mathcal{T}(\Sigma)$  can also be represented by a collection of marked Riemann surfaces. More specifically, given a hyperbolic surface  $S$ , points in  $\mathcal{T}(\Sigma)$  are of the form  $[(S, h)]$ , where  $h : \Sigma \rightarrow S$  is an orientation-preserving homeomorphism, and  $(S, h_1) \sim (S, h_2)$  if  $h_1$  and  $h_2$  are isotopic. A commonly used analogy views  $\Sigma$  as an undressed body,  $S$  as the “clothing” for the body (which is fitting since we will discuss pants decompositions later), and  $h$  as a series of instructions for how to wear the clothes. For instance, one could obtain  $(S, h_2)$  from  $(S, h_1)$  by flipping a collar or smoothing a wrinkle, in which case  $(S, h_1) \sim (S, h_2)$ .

There are several ways to coordinatize  $\mathcal{T}(\Sigma)$ . One classical method is through *Fenchel-Nielsen coordinates*, which identify points in  $\mathcal{T}(\Sigma)$  with points in  $\mathbb{R}_+^{3g-3} \times \mathbb{R}^{3g-3}$ , a space with a more familiar topology. We provide a sketch of the identification, again omitting proofs of many statements, below.

**Theorem 4.3** (Fenchel-Nielsen).  *$\mathcal{T}(\Sigma)$  is homeomorphic to  $\mathbb{R}_+^{3g-3} \times \mathbb{R}^{3g-3}$ .*

Recall that a simple closed curve is a non-self-intersecting closed curve. A *pants decomposition* is a partition of a hyperbolic surface into three-holed spheres  $(\Sigma_{0,3})$ , but it can also be thought of as a maximal collection of disjoint, non-parallel and homotopically non-trivial simple closed curves (see figure 8). Recall that on any closed surface, every non-trivial curve is homotopic to a closed geodesic. If we require the surface to be hyperbolic, the closed geodesic becomes unique. As a result, every hyperbolic surface  $\Sigma_{g,0}$  can be divided by  $3g - 3$  simple closed curves into  $2g - 2$  pairs of pants. Furthermore, we can equip every pair of pants with a hyperbolic metric such that every boundary component is a closed geodesic.

Recall if we lift two disjoint closed geodesics to the hyperbolic plane, and they do not meet at  $\partial\mathbb{H}^2$ , there is always a unique perpendicular between them. As a result, we can cut along the “seams” of a pair of pants, which are the unique perpendicular arcs between the boundary components. We then obtain two right-angled hexagons uniquely determined by measuring every other side length (see figure 9).

We can specify these three side lengths arbitrarily and reglue the surface back together, and then specify the hyperbolic metric on each pair of pants so that adjacent “cuff lengths” agree. The collection of pairs of pants, along with their hyperbolic metrics, determines a unique hyperbolic metric that, when restricted to

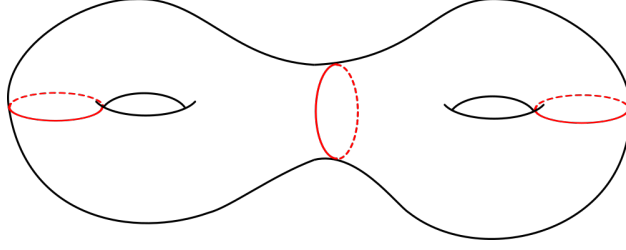


Figure 8: The pants decomposition of  $\Sigma_{2,0}$ . Note that the red pants curves form a maximal set of non-parallel, nontrivial simple closed curves on the surface.

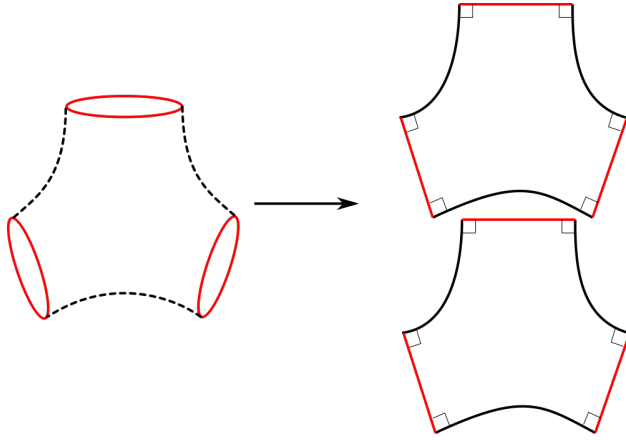


Figure 9: If we cut along the “seams” of each pair of pants (the dotted black lines), we obtain two right-angled hexagons that are uniquely determined by specifying every other side length. In particular, we can specify the lengths of the red pants curves.

each pair of pants, agrees with the locally assigned metric. Furthermore, in order to represent every hyperbolic metric, one can specify an additional “twist” coordinate on every boundary component, which gives instructions on how to glue adjacent pants together so that the “seams” are offset. The twist coordinate, unlike the length coordinate, can be negative. Altogether, the length and twist coordinates equip each pants decomposition with  $(3g - 3) * 2 = 6g - 6$  choices of values. We have then identified hyperbolic metrics with points in  $\mathbb{R}_+^{3g-3} \times \mathbb{R}^{3g-3}$ .

#### 4.2.2 Using Fenchel-Nielsen coordinates to prove Penner-Harer’s theorems

The upshot of this discussion is that a choice of  $\epsilon$ , along with a hyperbolic metric, determines the train track suited to a lamination. We can construct a train track from a geodesic lamination  $\mathcal{L}$  by choosing an  $\epsilon$  and identifying all leaves of  $\mathcal{L}$  that are distance  $\epsilon$  apart with respect to the fixed hyperbolic metric (see figure 10).

Dually, if one fixes a sufficiently small  $\epsilon$  and changes the metric, one would also obtain train tracks that differ by splits and folds (see figure 11).

Thus, given an appropriately small  $\epsilon$ , the hyperbolic metric determines a train track that a lamination is suited to. We can therefore identify each element of an equivalence class of train tracks with a hyperbolic metric, which corresponds to a point in  $\mathcal{T}(S)$ . Fenchel-Nielsen coordinates then allow us to interpolate between two different metrics- and two equivalent train tracks- by changing cuff lengths or twist coordinates.

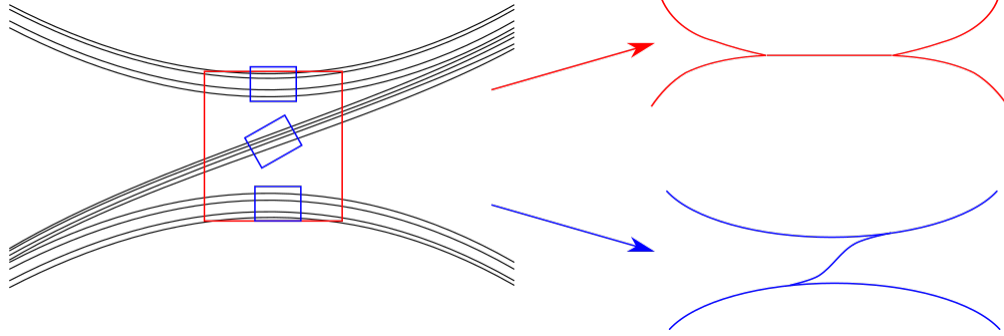


Figure 10: Different choices of  $\epsilon$ -neighborhoods will yield different train tracks. In this case, if the hyperbolic metric is fixed and we vary  $\epsilon$ , choosing the red  $\epsilon$ -neighborhood yields a folded version of the train track obtained by choosing the blue  $\epsilon$ -neighborhood.

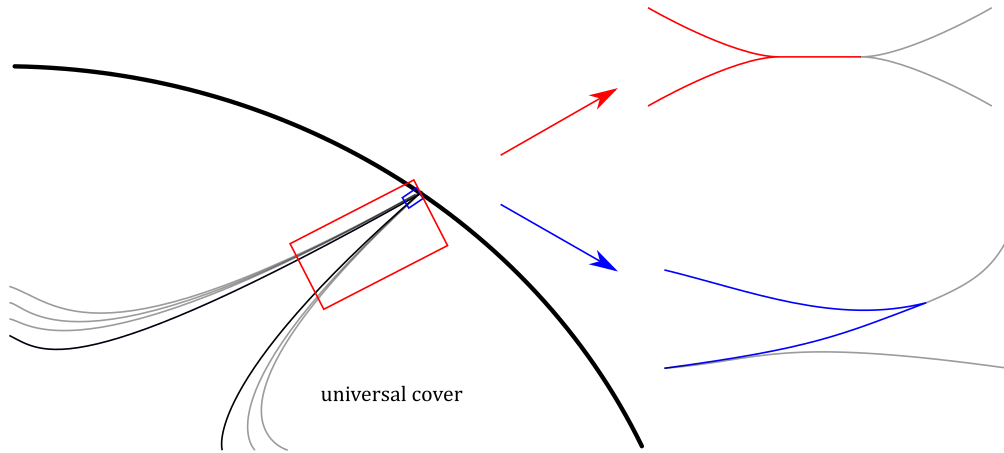


Figure 11: A choice of metric affects how the half-leaves adjacent to an ideal vertex (shown in black) are identified in the universal cover. Assume  $\epsilon$  is fixed. Clearly, the red metric identifies more of the two half-leaves than the blue metric, yielding a folded version of the train track obtained from the blue metric.

We now return to our original statements. Consider a lamination  $\mathcal{L}$ , which is suited to  $(\tau_1, \mu_1)$  and  $(\tau_2, \mu_2)$  by the carrying maps  $f_1$  and  $f_2$ . We can describe  $f_1$  and  $f_2$  by fixing a small enough  $\epsilon$  and choosing two appropriate hyperbolic metrics. Each metric is identified with a train track that differs from the other by splits or folds. As a result,  $(\tau_1, \mu_1) \sim (\tau_2, \mu_2)$ .

Conversely, suppose  $\mathcal{L}$  is suited to  $(\tau_1, \mu_1)$ , and  $(\tau_1, \mu_1) \sim (\tau_2, \mu_2)$ . We can fix a sufficiently small  $\epsilon$  and identify  $(\tau_1, \mu_1)$  with a metric. Since  $(\tau_1, \mu_1)$  and  $(\tau_2, \mu_2)$  differ by a series of splits and folds, we can associate each intermediate train track with a hyperbolic metric to create a continuous path of metrics. As a result, we can represent  $(\tau_2, \mu_2)$  by a hyperbolic metric, which is associated with a carrying map. Then  $\mathcal{L}$  is suited to  $(\tau_2, \mu_2)$ , as desired.  $\square$

### 4.3 Proof of the main theorem

We are now ready to generalize the main theorem from [2] to our case of orbifold train tracks.

**Theorem 4.4.** *Suppose  $\varphi : \Sigma_{0,n}/\Gamma \rightarrow \Sigma_{0,n}/\Gamma$  is pseudo-Anosov with stable lamination  $\mathcal{L}^s$ . Suppose  $(\tau, \mu)$*



is suited to  $\mathcal{L}^s$ . Then  $\exists$  some  $n, m$  st

$$(\tau, \mu) \stackrel{n}{\prec} (\tau_n, \mu_n) \stackrel{m}{\prec} (\tau_{n+m}, \mu_{n+m}) = (\varphi(\tau_n), \varphi_*(\mu_n))$$

Before we prove this theorem, there are some lemmas to prove. The first lemma ensures that any large branch of a train track will eventually be split in an infinite maximal splitting sequence.

A lamination  $\mathcal{L}$  is minimal if its half-leaves form a dense set; in other words, the closure of each half-leaf is the entire lamination.

A *trainpath* is a differentiable immersion  $\rho : [m, n] \rightarrow \tau \subset S/\Gamma$  that maps intervals  $[k, k+1]$ ,  $k \in [m, n-1]$ , onto branches of  $\tau$ . We call  $n - m$  the length of  $\rho$ . Following this terminology, we first show that given any branch  $e$  of  $\tau$ ,  $e$  must eventually be split in a maximal splitting sequence.

**Lemma 4.5.** *Let  $\mathcal{L}$  be a minimal lamination suited to  $(\tau, \mu)$ . Suppose  $(\tau_1, \mu_1) \prec (\tau_2, \mu_2) \prec \dots \prec (\tau_n, \mu_n) \prec \dots$  is an infinite sequence of maximal splittings. Then for any branch  $e \subset \tau$ , there exists some  $n$  st  $(\tau_n, \mu_n) \prec (\tau_{n+1}, \mu_{n+1})$  splits  $e$ . In other words,  $\mu_n(e)$  is a branch of maximal weight in  $\tau_n$ .*

*Proof.* Since  $\mathcal{L}$  is suited to  $(\tau, \mu)$ , by definition, we know that for some differentiable  $f : S_{0,n}/\Gamma \rightarrow S_{0,n}/\Gamma$ ,  $f(\mathcal{L}) = \tau$ . Take a half-leaf,  $l \subset \mathcal{L}$ . Because  $\mathcal{L}$  is minimal,  $e \subset \tau = f(\bar{l}) \subseteq \overline{f(l)}$ . Then it must follow that  $f(l)$  must cross  $e$  since  $l$  is an infinite ray. At each cusp,  $c$ , the two half leaves, denoted  $l_1, l_2$ , that lift to boundaries of an ideal polygon corresponding to a complementary region of  $\mathcal{L}$  on the universal cover, remain asymptotic to but disjoint from each other along the branch adjacent to  $c$  (see figure 12). Note that  $l_1$  and  $l_2$  cannot join to become an isolated monogon around an orbifold point; in that case, they would not be disjoint. Then  $f(l_1)$  and  $f(l_2)$  will also be asymptotic to each other along this branch. For  $i = 1, 2$ , consider the trainpath  $\rho_{c,i} : [m_i, n_i] \rightarrow \tau$  that follows  $f(l_i)$ . We also require that  $\rho_{c,i}(m_i) = c$  and  $\rho_{c,i}(n_i) = e$ . Since every half-leaf is dense, its image crosses  $e$  eventually, so we can assume such trainpaths exist.

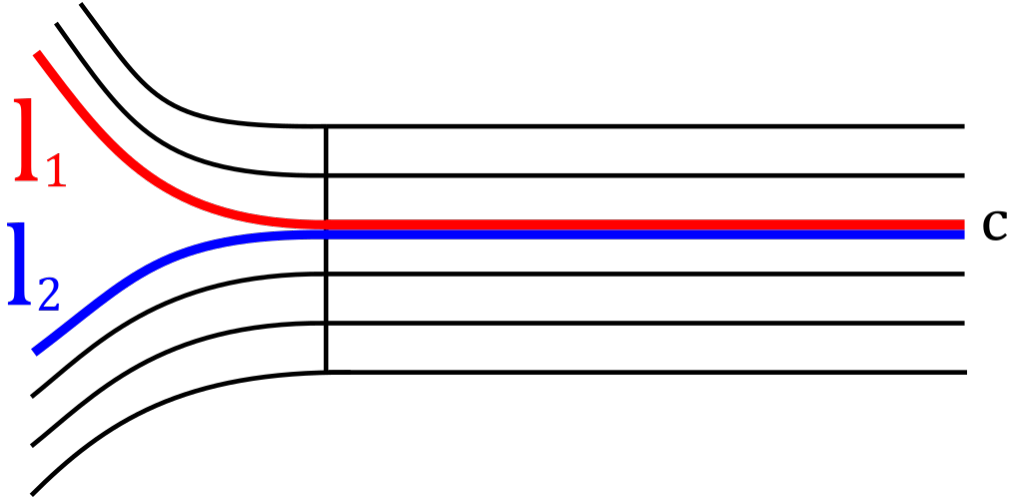


Figure 12:  $l_1$  and  $l_2$  are half-leaves both emanating from the cusp  $c$ . Along the edge adjacent to  $c$ , they are asymptotic in the sense that their lifts to the universal cover only "intersect" past points at infinity.

Apply a split on the branch adjacent to  $c$  and notice that  $\rho_{c,2}$  shrinks in length from  $n_2 - m_2$  to  $n_2 - (m_2 + k)$ , where  $k$  denotes the number of times  $\rho_{c,2}$  crosses the split branch, while  $\rho_{c,1}$  remains the same in length, or vice versa, depending on the weights (see figure 13). As a result, the sum of the lengths of  $\rho_{c,i}$  for  $i = 1, 2$  decreases by at least 1 when the branch adjacent to  $c$ , denoted  $b$ , splits. Repeat the argument

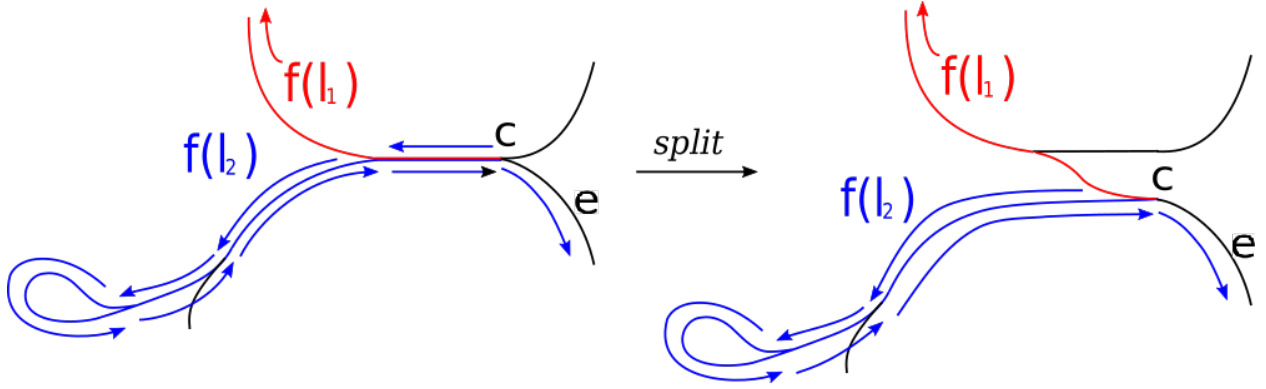


Figure 13: In this diagram,  $\rho_{c,2}$  shrinks in length from 8 to 6 while  $\rho_{c,1}$  stays the same length.

with the other cusp  $c'$  adjacent to  $b$  and note that the sum of the lengths of  $\rho_{c',i}$  for  $i = 1, 2$  also decreases by at least 1 when  $b$  is split. Consider the sum of all such trainpaths for every cusp of the train track and notice that during every split along the maximal splitting sequence, the sum of all cusp paths decreases by at least 2. By induction, this sum eventually becomes either 1 or 0, in which case  $e$  must have been split in the sequence.

In Figure 14, we illustrate the argument in the previous paragraph for orbifolds. In this example, the large branch in question undergoes the orbifold split-shift sequence, defined in Section 3, reserved for branches adjacent to isolated monogons surrounding orbifold points.

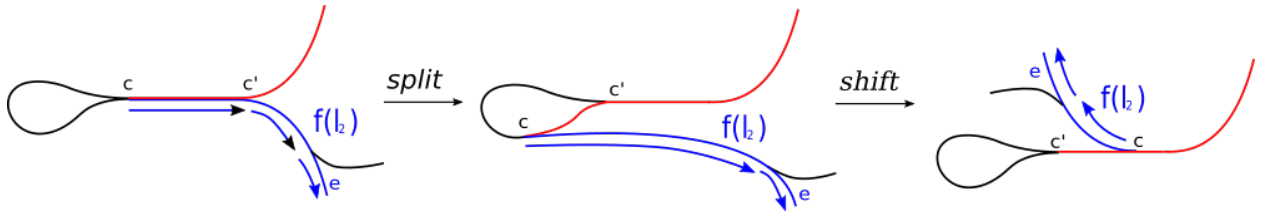


Figure 14: We see that after a split-shift combination we used to define splits of large branches adjacent to isolated monogons around orbifold points,  $\rho_{c,2}$  also shrinks in size by at least 1 in the orbifold case.

The only discrepancy is that, as mentioned before, there are no pairs of disjoint, asymptotic leaves emanating from  $c'$ , the cusp adjacent to  $c$ , so one need not consider cusp paths originating from  $c'$ . Figure 15 illustrates some issues that arise when one considers cusp paths from  $c'$ . In short, after the split-shift sequence, the new trainpath is no longer differentiable.

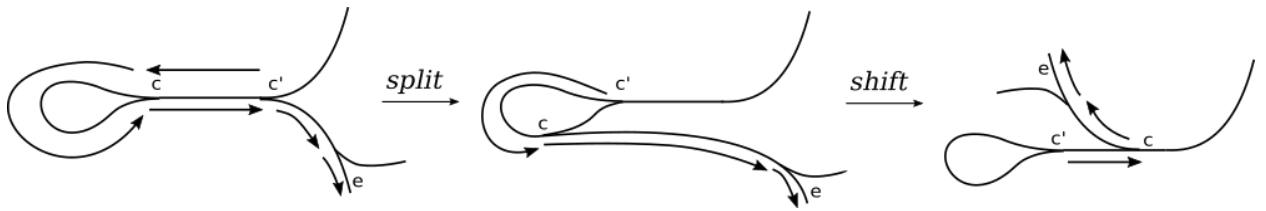


Figure 15: If we do indeed consider the cusp path from  $c'$ , we would obtain an illegal trainpath after the split-shift sequence.

□

Two train tracks  $(\tau, \mu)$  and  $(\tau', \mu')$  have a *common splitting*  $(\tau'', \mu'')$  if one can obtain  $(\tau'', \mu'')$  through some sequence of splits on  $(\tau, \mu)$  and  $(\tau', \mu')$ . The following lemmas show that having a maximal common splitting is an equivalence relation, and that two equivalent train tracks always share a common maximal splitting.

**Lemma 4.6.** *Having a common maximal splitting is an equivalence relation.*

*Proof.* Reflexivity and symmetry are clear. The only nontrivial condition is transitivity. The proof of this lemma relies on the fact that the common maximal splitting sequence is canonical; in other words, there is only one way to split a train track maximally. Suppose that  $(\tau_1, \mu_1) \xrightarrow{m} (\tau', \mu')$ ,  $(\tau_2, \mu_2) \xrightarrow{m} (\tau', \mu')$ , and  $(\tau_2, \mu_2) \xrightarrow{n} (\tau'', \mu'')$ ,  $(\tau_3, \mu_3) \xrightarrow{n} (\tau'', \mu'')$ . Consider  $N = \max(m, n)$ . Notice that either  $(\tau', \mu') \xrightarrow{N-m} (\tau'', \mu'')$  or  $(\tau'', \mu'') \xrightarrow{N-n} (\tau', \mu')$ . In the first case,  $(\tau_1, \mu_1) \xrightarrow{N} (\tau'', \mu'')$ , so  $(\tau'', \mu'')$  is the common maximal splitting of  $(\tau_1, \mu_1)$  and  $(\tau_3, \mu_3)$ . In the second case,  $(\tau_3, \mu_3) \xrightarrow{N} (\tau', \mu')$ , so  $(\tau', \mu')$  is the common maximal splitting of  $(\tau_1, \mu_1)$  and  $(\tau_3, \mu_3)$ . □

**Lemma 4.7.** *Let  $e$  be a large branch of nonmaximal weight. Then the two splittings  $(\tau, \mu) \xrightarrow{e} (\tau', \mu')$  and  $(\tau, \mu) \xrightarrow{1} (\tau'', \mu'')$  commute. In other words, the following diagram commutes.*

$$\begin{array}{ccc} (\tau'', \mu'') & \xrightarrow{\text{split } e} & (\tau''', \mu''') \\ \text{max split} \uparrow & & \text{max split} \uparrow \\ (\tau, \mu) & \xrightarrow{\text{split } e} & (\tau', \mu') \end{array}$$

Note that for any large branch  $e$ , a split cannot occur at the branches incident to  $e$ , denoted  $a, b, c, d$  since such branches will not be large. Moreover, if one splits along a branch incident to  $a, b, c$  or  $d$ ,  $\mu(a), \mu(b), \mu(c)$ , and  $\mu(d)$  will remain unchanged (see figures 16 and 17). One can easily imagine that if a split occurs even further away from  $e$ , or at branches not incident to  $a, b, c$ , or  $d$ , then  $\mu(a), \mu(b), \mu(c), \mu(d)$  will also remain unchanged. As a result, applying  $(\tau, \mu) \xrightarrow{1} (\tau'', \mu'')$ , regardless of where  $e$  is located relative to branches of maximal weight, will not affect how  $e$  is split.

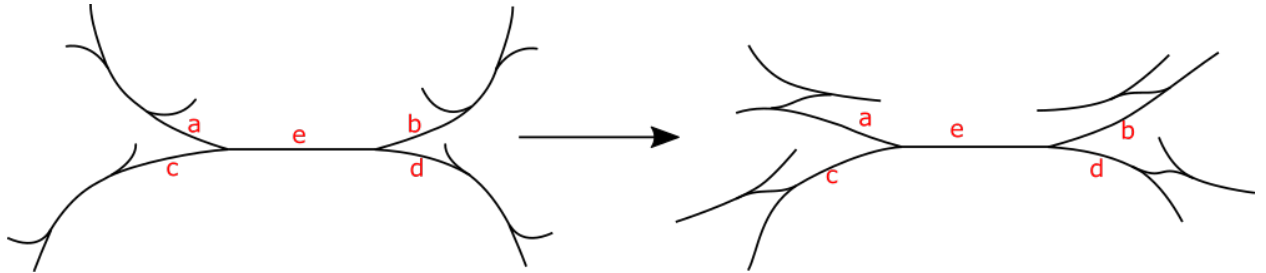


Figure 16: Splitting along branches incident to  $a, b, c, d$  do not affect  $\mu(a), \mu(b), \mu(c), \mu(d)$ .

*Proof.* We now show that splitting along  $e$  will not affect a maximal split. Refer to figure 18 to note that splitting along  $e$  to create  $e'$  will create at most two large branches, which we call  $b$  and  $c$ . However neither of which will be a branch of maximal weight  $\mu(b), \mu(c) < \mu(e) < \mu(m)$ , where  $m$  is a branch of maximal weight. As a result,  $(\tau, \mu) \xrightarrow{e} (\tau', \mu')$  will not affect a maximal split, as no new branches of maximal weight are produced. We conclude that splitting along a branch of nonmaximal weight,  $e$  will occur independently of a maximal splitting, so the splittings commute. □

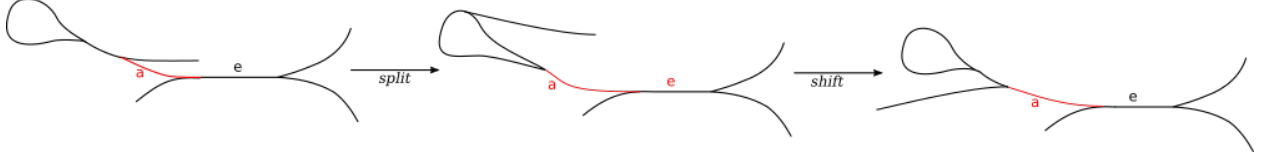


Figure 17: Even if one of the branches adjacent to  $e$ , ie,  $a$ , is adjacent to a large branch next to an isolated monogon around an orbifold point,  $\mu(a)$  is unaffected.

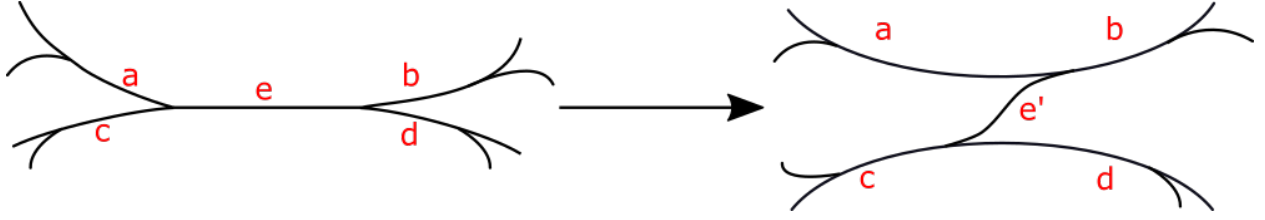


Figure 18: Splitting along  $e$  will not produce any branches of maximal weight.

**Lemma 4.8.** *We continue the notation from Lemma 4.7. Given a lamination  $\mathcal{L}$  suited to  $(\tau, \mu), (\tau', \mu')$ , there exists a maximal common splitting  $(\tau'', \mu'')$  where  $(\tau, \mu) \stackrel{max}{\prec} (\tau'', \mu'')$  and  $(\tau', \mu') \stackrel{max}{\prec} (\tau'', \mu'')$ .*

*Proof.* By theorem 4.1, if  $\mathcal{L}$  is suited to  $(\tau, \mu)$  and  $(\tau', \mu')$ , then  $(\tau, \mu) \sim (\tau', \mu')$ . In other words,  $(\tau, \mu)$  and  $(\tau', \mu')$  differ by a series of splits, folds, and shifts. Recall from Lemma 4.6 that having a maximal common split is transitive. Thus, it suffices to consider the case in which one obtains  $(\tau', \mu')$  from one split, fold, or shift of  $(\tau, \mu)$ . We claim that this reduces to showing that given  $(\tau, \mu) \stackrel{e}{\prec} (\tau', \mu')$ , where  $e$  is some large branch of  $\tau$ ,  $\exists (\tau'', \mu'')$  where  $(\tau, \mu) \stackrel{max}{\prec} (\tau'', \mu'')$  and  $(\tau', \mu') \stackrel{max}{\prec} (\tau'', \mu'')$ . To see this, notice the cases of  $(\tau, \mu) \xrightarrow{fold} (\tau', \mu')$  and  $(\tau, \mu) \prec (\tau', \mu')$  are the same, since in both cases,  $(\tau, \mu)$  and  $(\tau', \mu')$  differ by a split; therefore, it would be enough to show two train tracks that differ by a split have a common maximal splitting. Consider the case where  $(\tau, \mu) \xrightarrow{shift} (\tau', \mu')$ . Refer to Figure 19 to deduce that  $(\tau, \mu)$  and  $(\tau', \mu')$  share a common splitting, denote  $(\tau''', \mu''')$ , obtained from splitting two branches of  $(\tau, \mu)$ . Again, since the property of having a common maximal splitting is transitive, it would suffice to show that  $(\tau, \mu), (\tau''', \mu''')$  and  $(\tau', \mu'), (\tau''', \mu''')$  share a common maximal splitting, which would follow by transitivity if we show train tracks that differ by one split have a common maximal splitting.

We point out that figure 19 only considers branches that are, in a sense, “far away” from isolated monogons around orbifold points. More precisely,  $b$  cannot be adjacent to an isolated monogon. Notice that if we attempt to shift such a  $b$ , and then split  $e$ ,  $b$  will not become a large branch. As a result,  $b$  cannot be split in order to yield a common maximal splitting (see figure 20).

Suppose  $(\tau, \mu) \stackrel{e}{\prec} (\tau', \mu')$ . There are three cases:  $e$  can be the sole branch of maximal weight, one of multiple branches of maximal weight, or neither. The first case is easy;  $(\tau', \mu')$  is the common maximal splitting since  $(\tau, \mu) \stackrel{e}{\prec} (\tau', \mu')$  is a maximal splitting sequence. Consider the second case. Let  $M$  be the set of branches of maximal weight  $\mu(e)$ ; note that  $e \in M$ . Then  $(\tau, \mu) \stackrel{1}{\prec} (\tau''_1, \mu''_1)$  splits  $M$  and  $(\tau', \mu') \stackrel{1}{\prec} (\tau''_2, \mu''_2)$  splits  $M \setminus \{e\}$  since  $e$  is no longer maximal in  $(\tau', \mu')$ . As a consequence,  $(\tau''_1, \mu''_1)$  is the common maximal splitting since  $(\tau, \mu) \stackrel{e}{\prec} (\tau', \mu') \stackrel{1}{\prec} (\tau''_2, \mu''_2)$  is a sequence that splits  $M = \{e\} \cup M \setminus \{e\}$ , so  $(\tau''_1, \mu''_1) = (\tau''_2, \mu''_2)$ .

Now consider the third case, where  $e$  is not a branch of maximal weight. By Lemma 4.5,  $\exists n$  st  $(\tau, \mu) \stackrel{n}{\prec} (\tau_n, \mu_n)$  splits  $e$ , as  $\mu_{n-1}(e)$  is the maximal weight of  $\mu_{n-1}$ . Suppose  $(\tau, \mu) \stackrel{i}{\prec} (\tau_i, \mu_i)$  and  $(\tau', \mu') \stackrel{i-1}{\prec} (\tau'_i, \mu'_i)$ . I claim that for all  $i = 2, \dots, n-1$ , we have that  $(\tau_i, \mu_i) \stackrel{e}{\prec} (\tau'_{i+1}, \mu'_{i+1})$ . Refer to

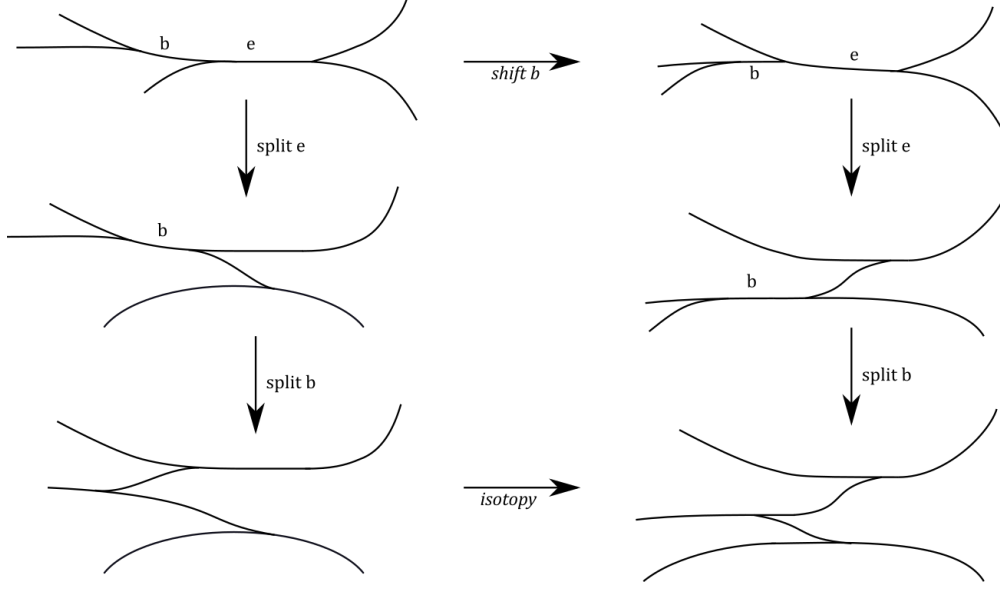


Figure 19: If two train tracks differ by a shift, they have a common splitting obtained from two splits.

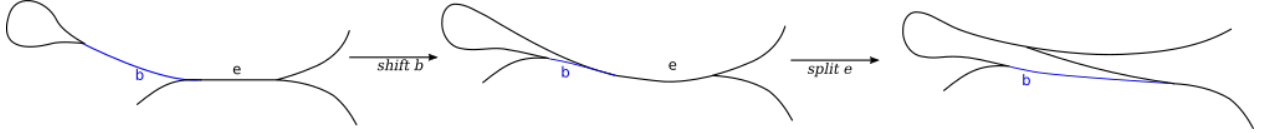


Figure 20: If  $b$  is next to an isolated monogon, then it will remain a mixed branch after one splits  $e$ . As a result, we do not allow  $b$  to be shifted.

figure 21 for a pictorial representation.

We use induction on  $i$ . The base case holds: by assumption  $(\tau, \mu) \stackrel{e}{\prec} (\tau', \mu') = (\tau'_1, \mu'_1)$ , where  $e$  is not maximal in  $\tau$ . Since  $e$  was assumed to be nonmaximal, by Lemma 4.7, the maximal split and the split along  $e$  commute. As a result, because  $(\tau, \mu) \stackrel{e}{\prec} (\tau', \mu') = (\tau'_1, \mu'_1) \stackrel{1}{\prec} (\tau'_2, \mu'_2)$ , we obtain  $(\tau, \mu) \stackrel{1}{\prec} (\tau_1, \mu_1) \stackrel{e}{\prec} (\tau'_2, \mu'_2)$ . Then  $(\tau_1, \mu_1) \stackrel{e}{\prec} (\tau'_2, \mu'_2)$ .

For the inductive step, assume  $(\tau_{i-1}, \mu_{i-1}) \stackrel{e}{\prec} (\tau'_i, \mu'_i)$ . Recall, again by Lemma 4.7, that the maximal split  $(\tau'_i, \mu'_i) \stackrel{1}{\prec} (\tau'_{i+1}, \mu'_{i+1})$  and  $(\tau_{i-1}, \mu_{i-1}) \stackrel{e}{\prec} (\tau'_i, \mu'_i)$  commute. If we know the splits commute, performing the maximal split on  $(\tau_{i-1}, \mu_{i-1})$  to obtain  $(\tau_i, \mu_i)$  and then splitting along  $e$  will also yield  $(\tau'_{i+1}, \mu'_{i+1})$ , which would imply that  $(\tau_i, \mu_i) \stackrel{e}{\prec} (\tau'_{i+1}, \mu'_{i+1})$ , as desired. In particular,  $(\tau_{n-1}, \mu_{n-1}) \stackrel{e}{\prec} (\tau'_n, \mu'_n)$ , and since  $e$  is now a branch of maximal weight, we can apply the same logic as in case 1 or 2 to deduce that  $(\tau_n, \mu_n) = (\tau'_{n+1}, \mu'_{n+1})$  is the common maximal split.

$$\begin{array}{ccc}
 (\tau'_i, \mu'_i) & \xrightarrow{\text{split } e} & (\tau'_{i+1}, \mu'_{i+1}) \\
 \text{max split} \uparrow & & \text{max split} \uparrow \\
 (\tau_{i-1}, \mu_{i-1}) & \xrightarrow{\text{split } e} & (\tau'_i, \mu'_i)
 \end{array}$$

□

We are now ready to prove Theorem 4.4.

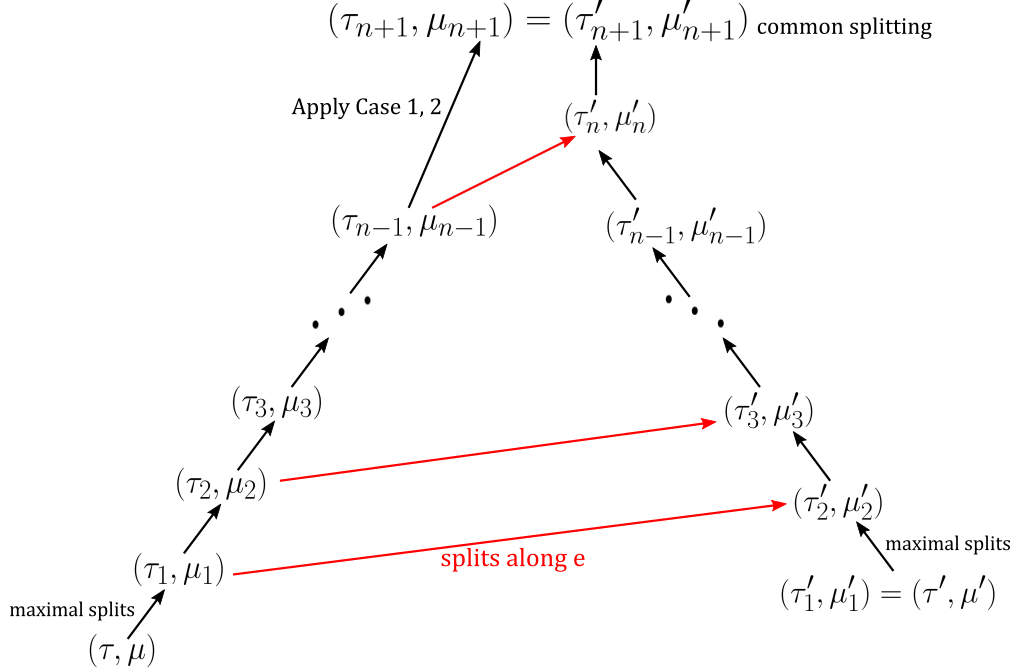


Figure 21: A splitting complex for the third case.

*Proof.* Suppose  $\varphi$  is a pseudo-Anosov map with stretch factor  $\lambda_\varphi$ , and  $(\tau, \mu)$  is suited to  $\mathcal{L}^s$ . By definition of a pA map,  $\varphi(\mathcal{L}^s) = \lambda_\varphi(\mathcal{L}^s) \implies \lambda_\varphi^{-1}\varphi(\mathcal{L}^s) = \mathcal{L}^s$ . In other words,  $\mathcal{L}^s$  is also suited to  $(\varphi(\tau), \lambda_\varphi^{-1}\varphi_*(\mu))$ . Suppose we have a maximal splitting sequence

$$(\tau, \mu) \prec (\tau_1, \mu_1) \prec \dots \prec (\tau_n, \mu_n) \prec \dots$$

Since the action of  $\varphi$  scales all the measures of  $\tau$  by the same factor, we have that maximal branches in  $(\tau_i, \mu_i)$  will still be maximal in  $(\varphi(\tau_i), \varphi_*(\mu_i))$ . For this reason,

$$(\varphi(\tau), \varphi_*(\mu)) \prec (\varphi(\tau_1), \varphi_*(\mu_1)) \prec \dots \prec (\varphi(\tau_n), \varphi_*(\mu_n)) \prec \dots$$

will still be a maximal splitting sequence. By theorem 4.2,  $\mathcal{L}^s$  is also suited to  $(\tau_n, \mu_n)$  since  $(\tau, \mu) \sim (\tau_n, \mu_n)$ . Since  $\mathcal{L}^s$  is suited to  $(\tau_n, \mu_n)$  and  $(\varphi(\tau), \lambda_\varphi^{-1}\varphi_*(\mu))$ , by Lemma 4.8, they share a common maximal splitting,  $(\varphi(\tau_n), \lambda_\varphi^{-1}\varphi_*(\mu_n)) = (\tau_{n+m}, \mu_{n+m})$ .  $\square$

## 5 A Worked Example

In order to demonstrate Theorem 4.4, we present a worked example based on the case of the 4-strand pseudo-Anosov braid of minimal dilatation presented in [2]. Instead of considering  $\Sigma_{0,5}$ , the 5-punctured sphere, we consider  $X$ , where the punctures of  $\Sigma_{0,5}$  are replaced by cone points. There is no canonical branched double cover. One possible manifold cover is the double torus  $\Sigma_{2,0}$ , as its quotient under an action of  $\mathbb{Z}_2 \times \mathbb{Z}_2$  yields  $X$ , so  $X$  is an orbifold. We can easily see that  $\Sigma_{2,0}$  is not a branched double cover; in particular, the points that are not cone points map homeomorphically to four distinct points on  $\Sigma_{2,0}$ . We consider the pseudo-Anosov map  $\varphi : X \rightarrow X$  where  $\mathcal{L}^s$  has 5 complementary regions that are monogons centered around cone points and one that is a triangle. Like the pseudo-Anosov described in [2],  $\varphi$  has stretch factor  $\lambda_\varphi = 2.29663\dots$

One can easily solve for the weights on the train track using systems of equations. We then obtain a weighted tree of monogons similar those described in [3] through a series of shifts and folds. Finally, we

show there is a periodic maximal splitting sequence such that after finitely many splits, all the weights of the branches are scaled by  $\lambda_\varphi^{-1}$ .

## 5.1 Creating a Tree of Monogons

Recall Agol's original train track, which consists of 5 monogons (with one around the point at infinity) and one trigon, on a 5-times punctured Riemann sphere [2]. Consider the point at infinity as a puncture. The resulting orbifold has an even number of singular points and thus lifts to  $\Sigma_{2,0}$ , the genus 2 surface whose quotient under the hyperelliptic involution is the sphere with 6 cone points. Considering the train track on its branched double cover,  $\Sigma_{2,0}$ , the monogons become bigons. As a result, the train track is, in a sense, not minimal, as bigons are not allowed in Agol's splitting sequence.

To circumvent this issue, we apply a series of folds and shifts on Agol's example of the train track representing the 4-stranded braid of minimal dilatation to obtain a tree of monogons (see figure 23).

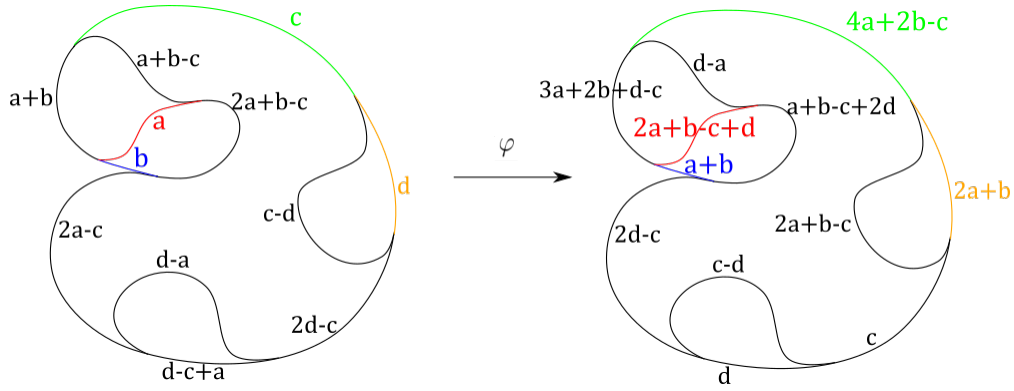


Figure 22: Calculating weights based on Agol's example.

In order to recover the weights for the tree, we construct a system of equations with 4 variables,  $a, b, c, d$  corresponding to the weights of 4 branches of the train track. Notice by figure 22 that determining the weights of these 4 branches determines the weights of all branches. Minimizing the number of variables in the system ensures against a singular system, thus making calculations on Matlab easier. We can see that following the action of  $\varphi$  on  $(\tau, \mu)$ , we obtain:

$$\varphi_*(a) = 2a + b - c + d; \quad (1)$$

$$\varphi_*(b) = a + b; \quad (2)$$

$$\varphi_*(c) = 4a + 2b - c; \quad (3)$$

$$\varphi_*(d) = 2a + b \quad (4)$$

which corresponds to the matrix  $\begin{bmatrix} 2 & 1 & -1 & 1 \\ 1 & 1 & 0 & 0 \\ 4 & 2 & -1 & 0 \\ 2 & 1 & 0 & 0 \end{bmatrix}$ . The eigenvector corresponding to the maximal eigenvalue,

2.29663, returns the maximal rescaled eigenvector  $\begin{bmatrix} 0.21463 \\ 0.16553 \\ 0.36086 \\ 0.25899 \end{bmatrix}$ . We then transfer the weights to our sequence

of shifts and folds (figure 23) and obtain a weighted tree of monogons. Refer to the starting tree of monogons in figure 24 for the resulting rescaled weighted tree.

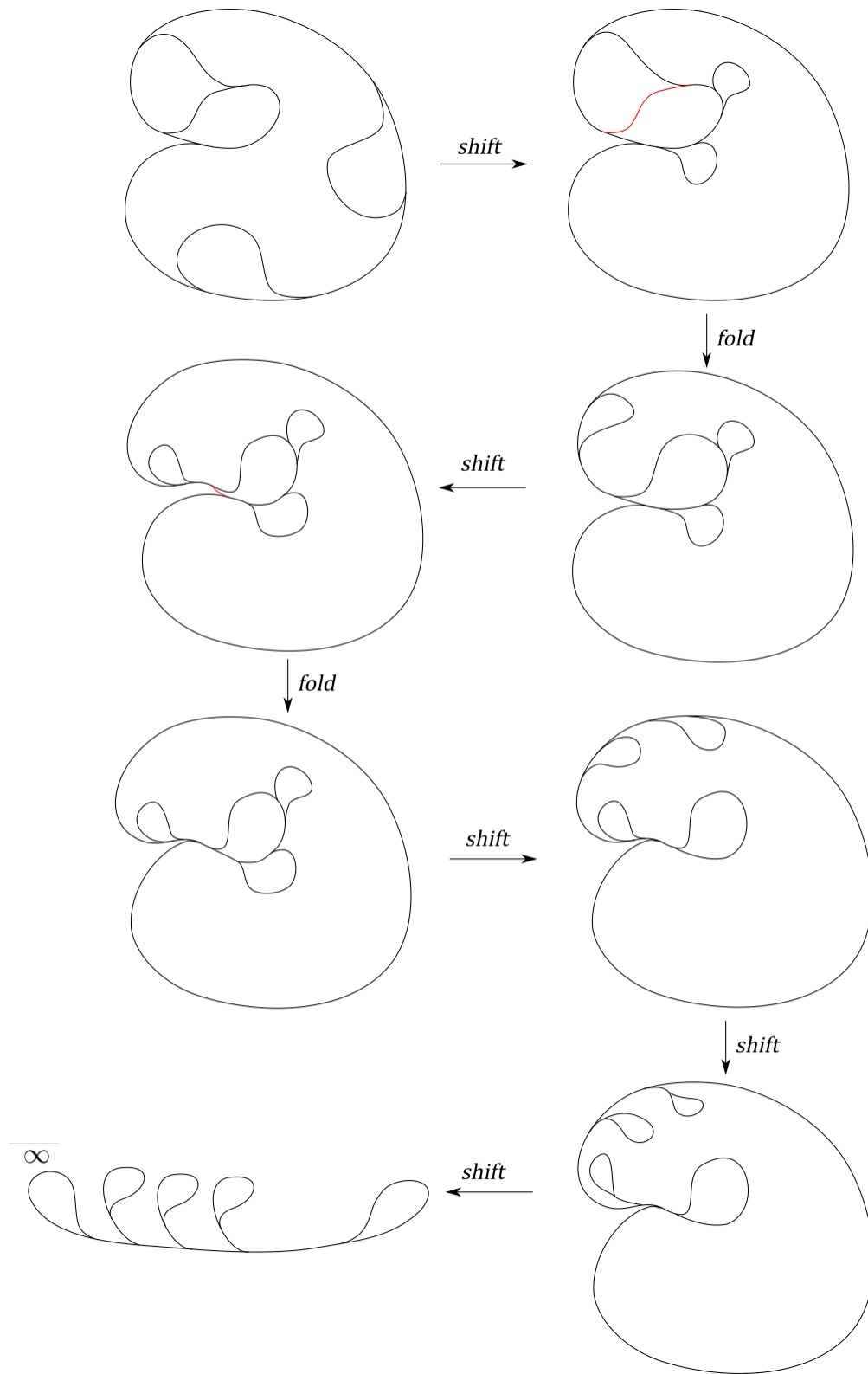


Figure 23: Creating a tree of monogons from splits and shifts. The final tree sits on a Riemann sphere.



## 5.2 Periodic Splitting Sequence and Splitting Automata

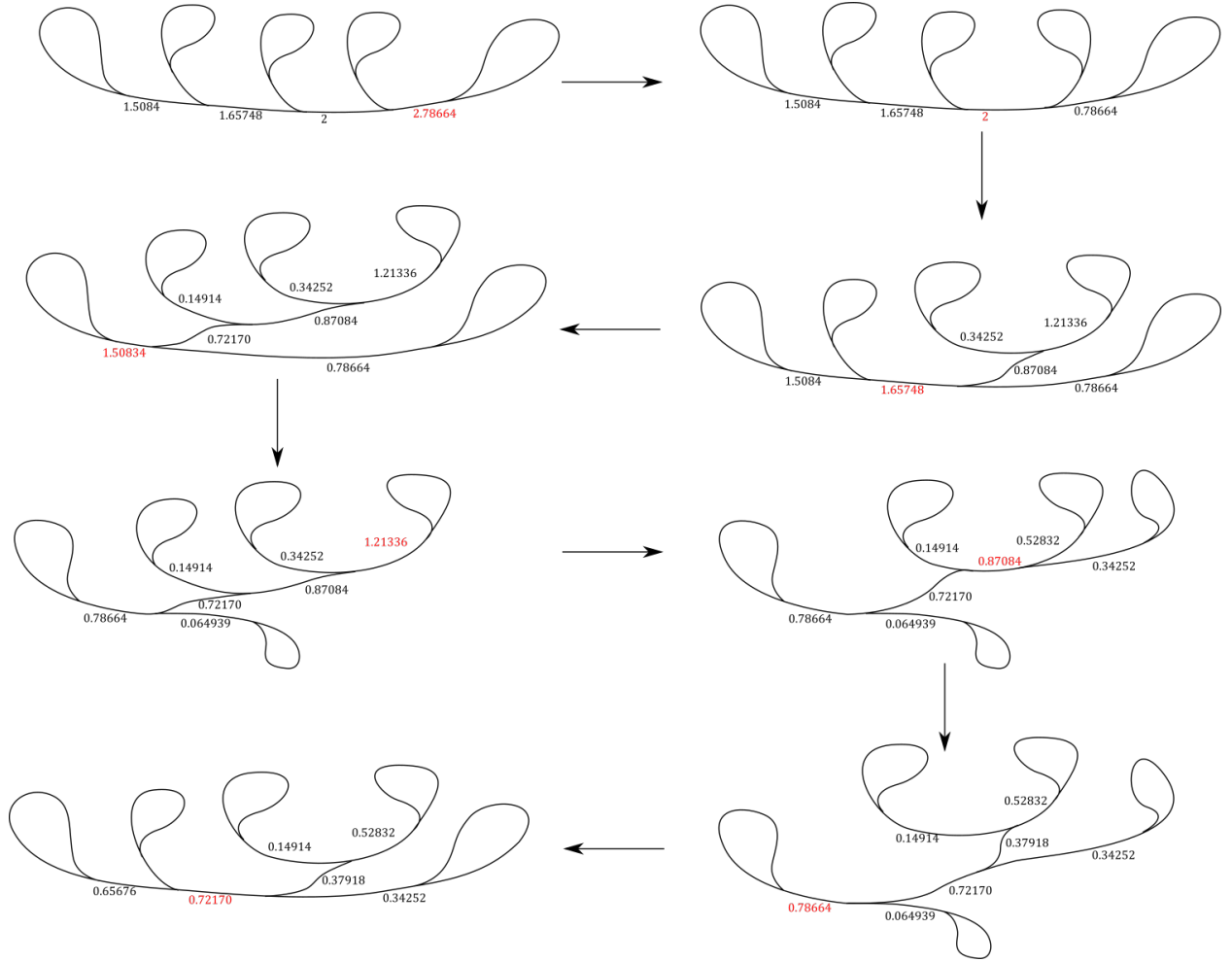


Figure 24: Eventually, a maximal splitting sequence is periodic modulo the action of  $\varphi$ . The weights are rescaled by  $\lambda_\varphi^{-1}$ .

Refer to Figure 24. Suppose we call the original train track  $(\tau, \mu)$  and denote  $(\tau, \mu) \xrightarrow{k} (\tau_k, \mu_k)$ . Note the train track obtained after applying two maximal splits,  $(\tau_2, \mu_2)$ . We notice that  $(\tau_7, \mu_7) = (\tau_7, \lambda_\varphi^{-1}(\mu_2))$ . From Theorem 4.4, we deduce that  $\varphi(\tau_2) = \tau_7$  and  $\varphi_*(\mu_2) = \lambda_\varphi^{-1}(\mu_2)$ . Although we have not kept track of the mapping class group for this particular example, there are no non-trivial automorphisms of our train track. As a result, the dilatation uniquely determines the mapping class group.

A *splitting automata* of a train track is a directed graph in which the vertices are train tracks, and the edges denote splits. A pair of commuting splits would form the edges of a square. As a result, an automata in which all splits commute will form a cube complex. In figure 25, we present the splitting automata of the same example explored previously. The automata contains 12 vertices and 19 edges, and 8 faces and is clearly a cube complex, as all the splits commute. Its Euler characteristic is 1, which is the same as that of a circle. As a result, the automata we obtain is homotopic to a circle.

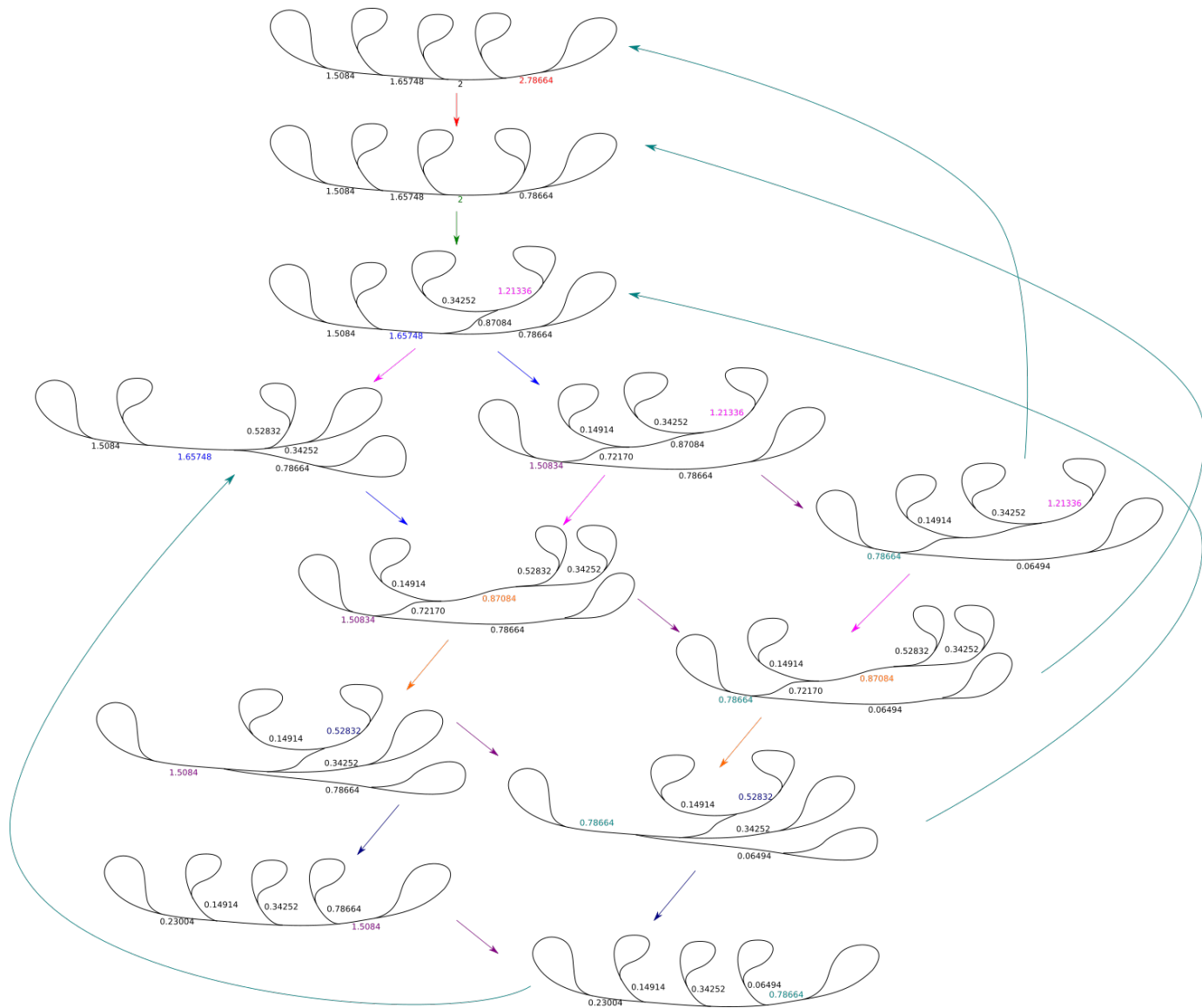


Figure 25: The full splitting automata. In particular, the teal arrows yield previously seen train tracks with weights scaled by a factor of  $\lambda_\phi^{-1}$ .

## 6 Future Directions

At the conclusion of this project, there are several unresolved questions. The first few arise from attempts to generalize Theorems 4.1 and 4.2 to orbifolds.

First, consider a lamination on an orbifold. Changing the cuff length and twist coordinates may drastically affect the lamination, constructed from geodesics of the new hyperbolic metric. As a result, one cannot concoct a neat set of rules that associate a change in cuff length or degree of twisting with a fold, shift, or split of the original train track, as a change in metric will affect the new lamination globally. It would be interesting, although unlikely, if one could take a sequence of splits, shifts, and folds and output a list of instructions on how to alter cuff length or degree of twisting.

One can also approach the proof of Penner-Harer’s theorems from the standpoint of ideal triangulations. Two ideal triangulations of a punctured surface are related by Whitehead moves. By relating a train track obtained from a stable lamination of a pseudo-Anosov to a dual spine of the triangulation, one can relate splits and folds to Whitehead moves. As a result, one could theoretically connect a folding and splitting sequence to a continuous sequence of Whitehead moves and provide a combinatorial approach to proving Penner-Harer’s theorems. A small caveat is that ideal triangulations are not well-defined on orbifolds, although there is an “obvious” way to define them. Given an orbifold, one could again consider an ideal triangulation of its branched double manifold cover, and then take the quotient of the triangulation by a group action to obtain an appropriate orbifold ideal triangulation.

Finally, revisiting the example in section 5, one notices all the splits commute, yielding a splitting complex homotopic to a circle. Hamenstadt shows that the splitting complex, a directed graph with train tracks as vertices and splits as edges, is  $CAT(0)$  in the manifold case. One could then explore whether this holds true in the orbifold context. Although it is still unclear to the author of this paper why such splitting automata are useful, it is possible there are connections to the study of braids applied to the orbits of planets and physical problems such as the Three Body Problem. Additionally, the splitting automata could somehow be useful in connecting the Garside solution to the word problem to the Nielsen-Thurston solution.

## References

- [1] Benson Farb, Christopher J. Leininger, Dan Margalit, *Small dilatation pseudo-Anosovs and 3-manifolds*, 40 pages, May 2000, [arXiv:0905.0219](https://arxiv.org/abs/0905.0219).
- [2] Ian Agol, *Ideal Triangulations of pseudo-Anosov mapping tori*, 16 pages, Contemporary Mathematics **560** (2011), [arXiv:1008.1606](https://arxiv.org/abs/1008.1606).
- [3] Eriko Hironaka and Eiko Kin, *A family of pseudo-Anosov braids with small dilatation*, Algebr. Geom. Topol. **6** (2006), 699-738, [arXiv:0904.0594](https://arxiv.org/abs/0904.0594).
- [4] Dan Peterson, stackoverflow, <https://mathoverflow.net/questions/105878/how-should-one-understand-orbifold-fundamental-groups>, August 30, 2012.
- [5] R.C. Penner and J.L. Harer, *Combinatorics of Train Tracks*, Annals of Mathematics Studies, vol. 125, Princeton University Press, Princeton, NJ, 1992.
- [6] Marc Lackenby, *Taut ideal triangulations of 3-manifolds*, Geom. Top. **4** (2000), 369-395 (electronic), [arxiv:0003132](https://arxiv.org/abs/0003132).
- [7] Feng Zhu, *Notes*, <http://www-personal.umich.edu/~zhufeng/notes.html>, updated December 27, 2017, accessed May 2018.